Journal of ELECTRONIC MATERIALS, Vol. 44, No. 11, 2015
DOI: 10.1007/s11664-015-3935-x
© 2015 The Minerals, Metals & Materials Society

CrossMark

Bipolar Switching Behavior of ZnO_x Thin Films Deposited by Metalorganic Chemical Vapor Deposition at Various Growth Temperatures

SEONHO BAE,[1] DAE-SIK KIM,[1] SEOJOO JUNG,[1] WOO SEOP JEONG,[1] JEE EUN LEE,[1] SEUNGHEE CHO,[1] JUNSUNG PARK,[1] and DONGJIN BYUN[1,2]

1.—Department of Materials Science and Engineering, Korea University, Anam-dong, Seongbuk-gu, Seoul 136-713, Republic of Korea. 2.—e-mail: dbyun@korea.ac.kr

The bipolar resistive switching behaviors of ZnO films grown at various temperatures by metalorganic chemical vapor deposition have been investigated. The ZnO films were grown on $Pt/Ti/SiO_2/Si(100)$ substrate, and the ZnO growth temperature was varied from 300°C to 500°C in steps of 100°C. Rutherford backscattering spectroscopy analysis results showed that the chemical compositions of the ZnO films were oxygen-poor $Zn_1O_{0.9}$ at 300°C, stoichiometric Zn_1O_1 at 400°C, and oxygen-rich $Zn_1O_{1.3}$ at 500°C. Resistive switching properties were observed in the ZnO films grown at 300°C and 400°C. In contrast, high current, without switching properties, was found in the ZnO film grown at 500°C. The ZnO film grown at 500°C had higher concentration of both nonlattice oxygen (4.95%) and oxygen vacancy (3.23%) than those grown at 300°C or 400°C. The resistive switching behaviors of ZnO films are related to the ZnO growth temperature via the relative amount of oxygen vacancies in the film. Pt/ZnO/Pt devices showed asymmetric resistive switching with narrow dispersion of switching voltage.

Key words: ZnO, bipolar switching behavior, metalorganic chemical vapor deposition, Rutherford backscattering spectroscopy (RBS), x-ray photoelectron spectroscopy (XPS)

INTRODUCTION

Resistive random-access memory (ReRAM) has attracted attention for use in next-generation memory, due to the extensive demand for low power consumption, high speed, and high density.[1] A large variety of materials have been found to exhibit the resistive switching phenomenon, including perovskite oxides such as $Pr_{0.7}Ca_{0.3}MnO_3$[2] and binary transition-metal oxides such as NiO,[3] TiO_2,[4,5] and ZnO.[6–8]

Resistive switching between the high-resistance state (HRS) and the low-resistance state (LRS) has been attributed to the following three mechanisms: (1) formation and rupture of a filamentary conductive path consisting of oxygen vacancies or mobile ions,[5,9] (2) redox reaction accompanied by migration of cations and anions caused by the strong electric field (redox model),[5,8,10,11] and (3) the interface barrier system accompanied by the contact resistance and barrier height at the interface between the middle semiconductor layer and the electrode (interface barrier model).[11,12] Whereas the switching mechanism in ReRAM remains a matter of heated debate and controversy, the most plausible explanation is related to the formation and rupture of filaments.

Among the materials mentioned above, ZnO is a VI–II metal oxide semiconductor with a direct bandgap (E_g = 3.37 eV at 300 K) and a relatively large exciton binding energy (~60 meV). Due to its unique properties, ZnO is used in various devices such as optoelectronic applications,[13,14] field-effect transistors,[15] energy-harvesting applications,[16,17]

(Received April 28, 2015; accepted July 13, 2015; published online July 28, 2015)

and piezoelectric applications.[18,19] In addition, ZnO has been demonstrated to have good resistive switching characteristics in recent research.[20]

Many researchers have studied material growth methods such as sputtering,[3,5,7,8] and pulsed laser deposition.[2,6] However, these physical vapor deposition (PVD) methods have difficulty controlling precise thickness, especially for nanometer-thick films. Metalorganic chemical vapor deposition (MOCVD) has the advantage of producing high-quality ZnO films with precise thickness control, good thermal stability, and electrical conductivity. In this work, ZnO films deposited by MOCVD were evaluated.

By using MOCVD, the process can be simplified, the process time can be shortened according to the deposition rate, and control of the ZnO thickness can be facilitated. In industrial applications, the MOCVD method promises high throughput for large-scale production. To make use of these advantages properly, it is crucial to know the relationship between the film growth temperature and the switching characteristics. Therefore, this study was designed to investigate the growth temperature dependence of the bipolar switching behavior based on ZnO films deposited on $Pt/Ti/SiO_2/Si(100)$ by MOCVD.

EXPERIMENTAL PROCEDURES

ZnO films were grown on $Pt/Ti/SiO_2/Si(100)$ substrate using MOCVD. MOCVD was achieved using a cold wall and vertical flow reactor. Diethylzinc [DEZn, $Zn(C_2H_5)_2$] and oxygen gas (O_2, 99.995% purity) precursors were used, and DEZn was maintained at 10°C. Argon (Ar, 99.999% purity) at 30 sccm was used as carrier gas for the DEZn. Oxygen gas was introduced separately into the reaction chamber at 100 sccm. The precursor volumetric ratio of O_2 to DEZn was kept at 148:1. The working pressure was maintained at 2 Torr. Field-emission scanning electron microscopy (FE-SEM, Hitachi S-4800) was used to carry out structural analysis. Depth profiling by Auger electron spectroscopy (AES, Physical Electronics, Model PHI 680) was applied to confirm the collapse of the sample structure by diffusion or contamination. X-ray diffractometry (XRD, Rigaku D) with Cu K_α radiation operating at 40 kV and 200 mA was used to analyze the crystalline structure.

ZnO films were deposited in the temperature range of 300°C to 500°C for 10 min. Pt top electrode was deposited on films using conventional direct-current (DC) sputtering (Emitech K550). The 100-nm-thick Pt top electrode was patterned by using a shadow mask to form a 280-μm-diameter circle. The composition of the crystalline ZnO films was analyzed by Rutherford backscattering spectroscopy (RBS, NEC 2-MV tandem accelerator). Photoluminescence (PL) measurements were performed using a He-Cd laser at room temperature. Current–voltage (I–V) measurements were performed using a Keithley 2400 voltage sourcemeter. The set voltage and reset voltage were slightly different. A current compliance is often used to avoid permanent breakdown in the set process. However, this is unnecessary in the reset process. The chemical bonding states of the ZnO films and the Pt top electrode were investigated by x-ray photoelectron spectroscopy [XPS, PHI 5000 Versa probe (Ulvac-PHI), monochromated Al K_α (1486.6 eV) anode (25 W, 15 kV)]. The C 1s peak position was taken as calibration standard with a binding energy of 284.8 eV. The fitting program Multi Pack (V.9.1.0.9., Ulvac-PHI, Inc.) was used. All measurements were performed at room temperature.

RESULTS AND DISCUSSION

Structure Analysis

Figure 1a shows a cross-sectional SEM image of the ZnO film grown at 400°C. The ZnO film was grown well with uniform thickness of 80 nm, and a sharp interface between the ZnO film and Pt electrode was observed. The thickness of the ZnO films grown at 300°C and 500°C was about 100 nm and 110 nm, respectively. An Auger depth profile of the as-deposited ZnO film on the Pt substrate is also illustrated in Fig. 1b. As shown in Fig. 1b, Pt ions did not diffuse into the ZnO film, and Zn and O ions also did not diffuse into the bottom and top Pt electrodes. Therefore, it was considered that the homogeneous ZnO film was well formed on the $Pt/Ti/SiO_2/Si$ substrate.

Figure 2 shows the logarithmic-scaled data of XRD ω–2θ scans of the ZnO films to confirm their epitaxial growth and single-crystalline nature. The crystalline ZnO peak with (002) preferred orientation was observed. Such c-axis preferential growth is common, since a (001) basal plane of ZnO crystals has the lowest surface energy. The full-width at half-maximum (FWHM) was 0.262°, 0.292°, and 0.613° for the ZnO films grown at 300°C, 400°C, and 500°C, respectively. These narrow FWHM values of the (002) peak indicate high crystal quality of the ZnO films. This result indicates that the ZnO films were grown well with wurtzite structure.

The RBS spectra of the ZnO films are shown in Fig. 3. The RBS data were measured by oxygen resonance energy. The chemical compositions of the ZnO films revealed 1:0.9, 1:1, and 1:1.3 ratio of Zn to O atoms at growth temperature of 300°C, 400°C, and 500°C, respectively. The ZnO film grown at 400°C had stoichiometric composition, whereas the ZnO films grown at 300°C and 500°C were nonstoichiometric and contained defects such as oxygen vacancies and interstitial oxygen ions. In particular, the ZnO film grown at 500°C deviated significantly from the stoichiometric composition.

PL was used to investigate the presence of defects. Figure 4 shows the PL spectra of the ZnO films. The strong ultraviolet (UV) peak at 378 nm corresponds to the near-band-edge (NBE) emission,

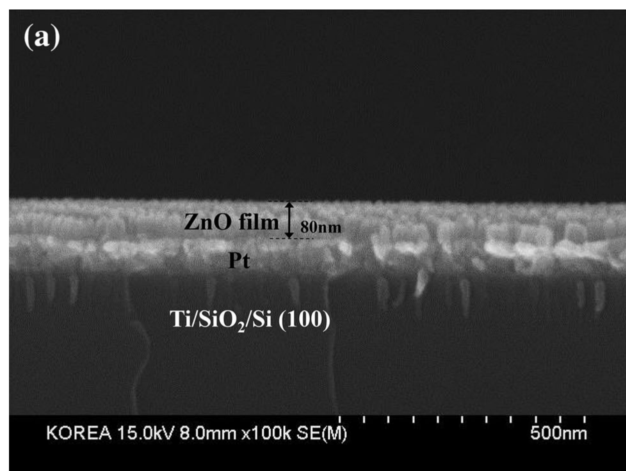

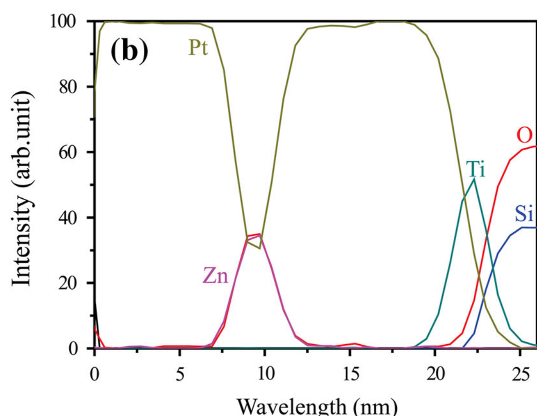

Fig. 1. (a) Cross-sectional SEM image, (b) Auger depth profile of ZnO grown at 400°C.

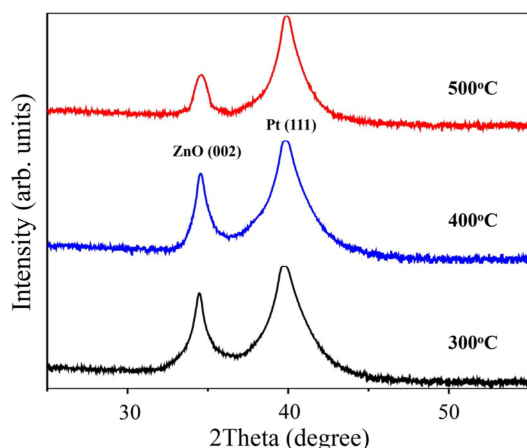

Fig. 2. XRD ω–2θ scans of the ZnO films showing (from the left) peaks of ZnO(002) and Pt(111) of samples prepared at 300°C, 400°C, and 500°C (logarithmic scaled).

while the weak luminescence at 510 nm was attributed to deep-level emission (DLE) due to a high density of native defects.[21] The peak at ~750 nm was related to the second-order feature of the NBE of ZnO. The stoichiometric ZnO film grown

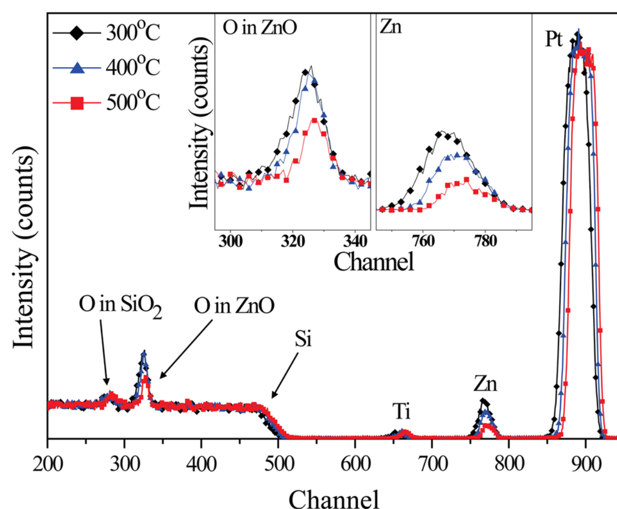

Fig. 3. RBS profiles of ZnO films deposited on $Pt/Ti/SiO_2/Si$ substrate at 300°C, 400°C, and 500°C. Oxygen in ZnO and Zn peaks are zoomed in the inset.

at 400°C showed strong NBE, while the nonstoichiometric ZnO films grown at 300°C and 500°C showed weak NBE and strong DLE relatively. The ratio of NBE to DLE (the PL ratio) was 1.47, 2.69, and 1.15 for the samples grown at 300°C, 400°C, and 500°C, respectively. The amount of defects in the ZnO films grown at 300°C and 500°C exceeded that in the ZnO film grown at 400°C, resulting in the strongest green light emission.[22] Therefore, the PL results implied that the ZnO films grown at 300°C and 500°C had some defects during MOCVD processing.

Characteristics Analysis

Figure 5 shows typical *I*–*V* characteristics of the Pt/ZnO/Pt devices grown at various temperatures. The voltage bias was scanned over the following voltage cycle: 0 V → +3 V → 0 V → –2 V → 0 V. The ZnO films grown at 300°C and 400°C exhibited asymmetric bipolar resistive switching behavior without an electrical forming process. The reason why no electrical forming process was needed can be attributed to the abundant oxygen vacancy clusters preexisting in the ZnO films, which cause the electrical forming voltage for the first HRS-to-LRS switching to be close to the set voltage.[7] Considering the *I*–*V* characteristics of the ZnO films grown at 300°C and 400°C, the current level of the latter film was higher than that of the former. When a voltage was applied to the Pt top electrode of the ZnO film grown at 400°C from zero to positive, the resistance decrease from the HRS to the LRS (set process) was observed at approximately 2.3 V. The sweeping starting at 2.3 V generated more conducting filaments driven by oxygen vacancies during the set process. As the voltage was applied from positive to zero, the LRS was maintained. In the sweep from zero to negative voltage, the resistance was increased from the LRS to the HRS (reset process) at

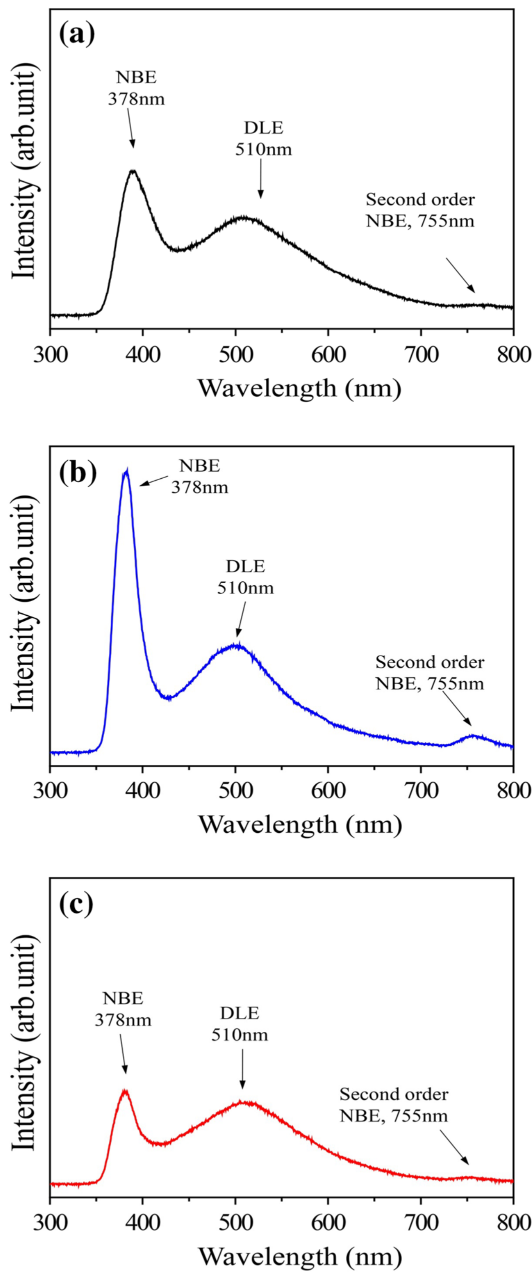

Fig. 4. Photoluminescence spectra (at 300 K) of aligned ZnO films grown at (a) 300°C, (b) 400°C, and (c) 500°C.

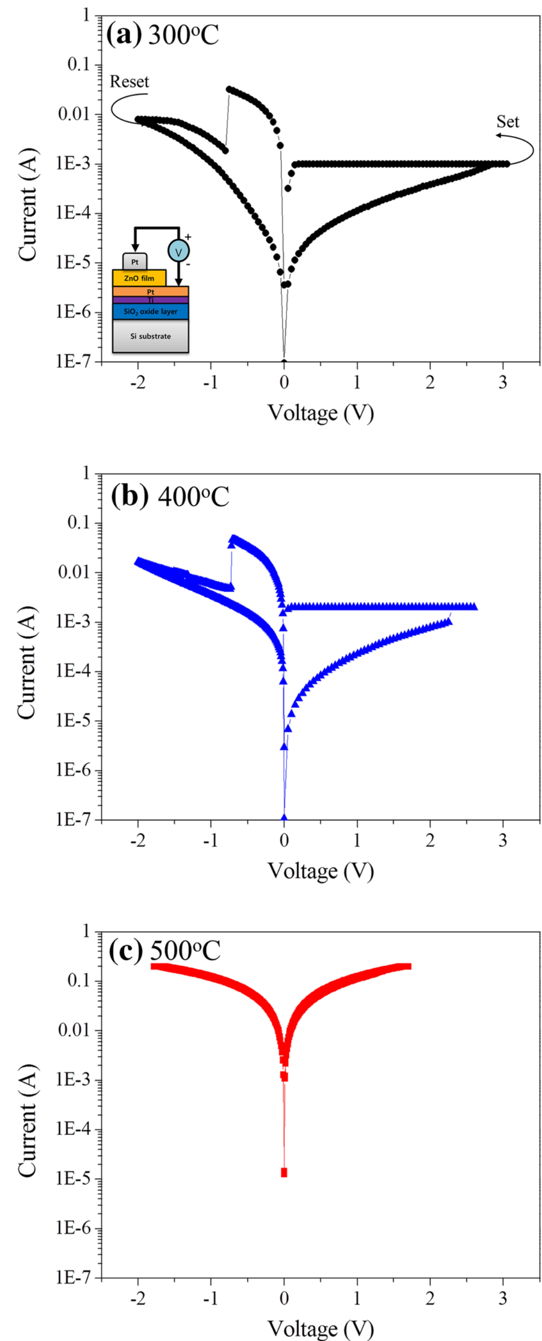

Fig. 5. Typical *I*–*V* characteristics of ZnO films grown at (a) 300°C, (b) 400°C, and (c) 500°C.

about −2.0 V. The conducting filaments constructed with oxygen vacancies were annihilated at this voltage. As the applied voltage was swept from negative to zero, the HRS was maintained. For the ZnO film grown at 300°C, the set and reset voltages were approximately 2.8 V and −2.0 V, respectively. However, switching behavior was not observed for the ZnO film grown at 500°C.

To investigate this phenomenon exactly, the chemical binding states of the fabricated ZnO films were studied by XPS, as shown in Fig. 6. Figure 6a–c shows XPS profiles of Zn $2p_{3/2}$ and O 1*s*. The Zn $2p_{3/2}$ spectrum shows a symmetric peak at binding energy of 1021.6 eV, corresponding to Zn^{2+} of a stoichiometric Zn–O bond.[23] The O 1*s* peak was asymmetrically shaped, and could be deconvoluted into three subpeaks at binding energy of ∼531 eV, ∼532 eV, and ∼533 eV. The three fit binding energy peaks approximated the results of Hsiteh et al.[24] The O_a component on the low-energy side of the O 1*s* spectrum at ∼531 eV was attributed to O^{2-} ions in the wurtzite structure of the hexagonal Zn^{2+} ion array, surrounded by Zn atoms with their full complement

of nearest-neighbor O^{2-} ions. The O_b binding energy component, centered at ~532 eV, was mainly caused by oxygen vacancies in oxygen-deficient regions. The high binding energy component O_c was associated with O^{2-} ions in chemisorbed or dissociated oxygen within the ZnO film, called nonlattice oxygen.[24,25] Therefore, changes in the intensity of these three components may be connected in part to the variations in the concentrations of lattice and nonlattice oxygen.

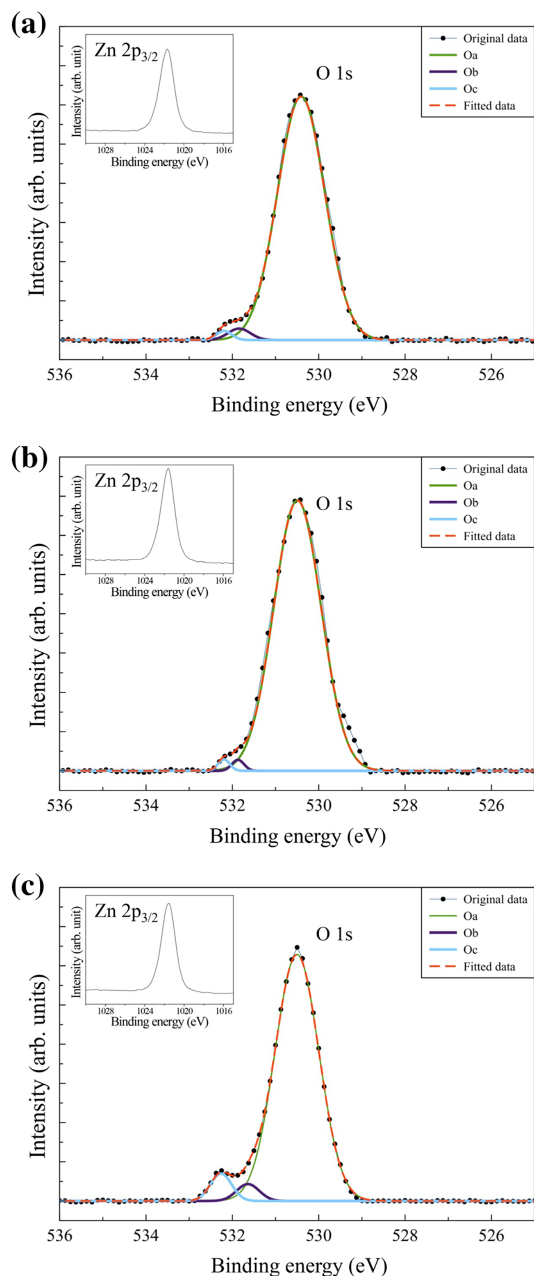

Fig. 6. XPS spectra of ZnO films grown at growth temperature of (a) 300°C, (b) 400°C, and (c) 500°C.

As shown in Table I, the relative intensity of the O^{2-} ions in the oxygen-deficient region (O_b species) was about 2.1%, 1.0%, and 3.2% for growth temperature of 300°C, 400°C, and 500°C, respectively. Meanwhile, the nonlattice oxygen percentage (O_c species) was approximately the same for growth at 300°C and 400°C, and highest at 500°C with a percentage of 4.95%. This result closely agrees with the chemical composition analysis showing an oxygen-rich composition of the ZnO film grown at 500°C (Fig. 2). On the other hand, the relative intensity of the O^{2-} ions in the wurtzite structure peak (O_a species) was approximately the same for growth at 300°C and 400°C, and lowest at 500°C. The reason why the O_a peak was lowest for growth at 500°C is presumably due to the increase of oxygen vacancies and nonlattice components. The conducting filaments in the ZnO films were formed by alignment of structural defects such as oxygen vacancies. So, a proper amount of oxygen vacancy defects is needed to observe switching behavior. The samples grown at 300°C and 400°C may have suitable amounts of oxygen vacancies for switching behavior. However, the ZnO film grown at 500°C had an excessive

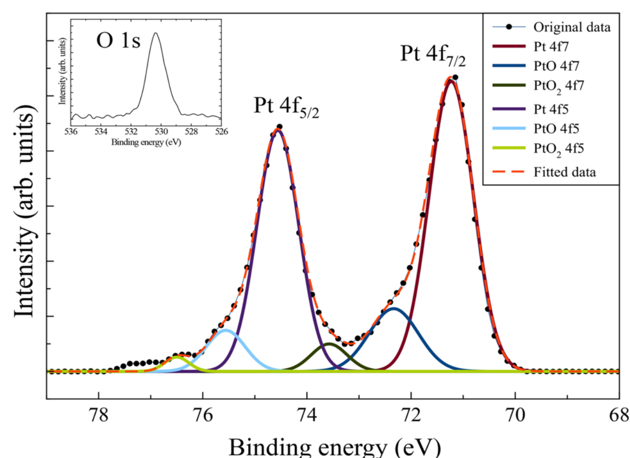

Fig. 7. XPS spectra of Pt 4*f* electrons from the Pt top electrode grown at 400°C. Insets show O 1*s* electron spectra for the top electrode surface.

Table I. Comparison of O 1*s* XPS data for ZnO samples grown at various temperatures

Growth Temperature (°C)	Peak O_a (eV)	O_a (%)	Peak O_b (eV)	O_b (%)	Peak O_c (eV)	O_c (%)
300	530.41	96.68	531.84	2.14	532.19	1.18
400	530.49	97.96	531.87	1.03	532.20	1.02
500	530.51	91.82	531.64	3.23	532.26	4.95

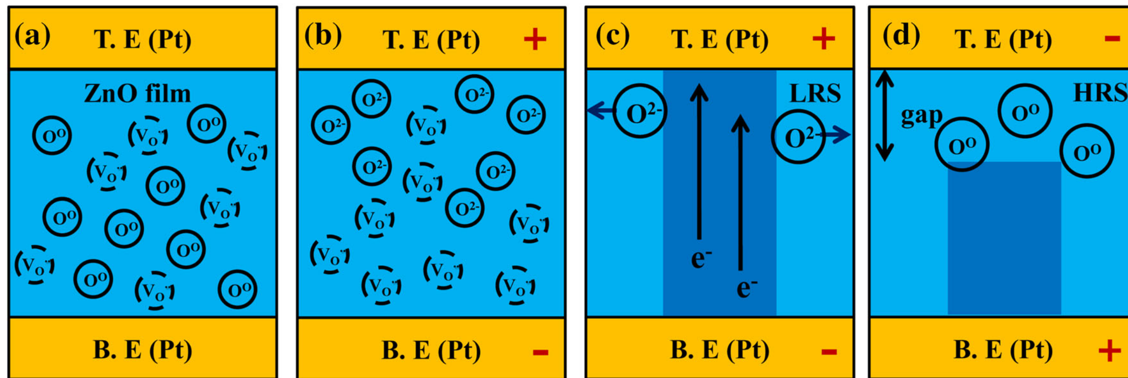

Fig. 8. Schematic diagram of the filament combined model in the ZnO film.

amount of oxygen vacancy defects, so the leakage current could easily flow through the defects in the ZnO. Therefore, no resistive switching behavior was observed for the ZnO film grown at 500°C.

Switching Mechanism

Figure 7 demonstrates the results of XPS analysis conducted on the ZnO film grown at 400°C to investigate the role of the Pt top electrode during the switching process. The Pt 4*f* peaks from the top electrode in the LRS were resolved into six peaks by Gaussian distribution fitting. These peaks correspond to the metallic state (Pt) and the oxidized states (PtO_{1+x}), as shown in Fig. 7. The metallic state (Pt) corresponds to the peaks at binding energy of 71.2 eV and 74.6 eV, whereas the oxidized states correspond to the peaks for PtO at 72.2 eV and 75.6 eV, and for PtO_2 at 73.6 eV and 76.5 eV.[26] The O 1*s* spectrum with the peak at binding energy of 530.4 eV also indicates oxygen incorporated with Pt.[27] These results suggest that the Pt top electrode behaved as an oxygen reservoir in the Pt/ZnO/Pt devices. Similar results were also observed in a Pt/NiO/TiN device.[28]

Based on these observations, we propose the following switching mechanism for the Pt/ZnO/Pt devices: The ZnO films contained zinc ions, oxygen ions, interstitial oxygen ions, and oxygen vacancies, according to their compositions (Fig. 8a). When a positive voltage bias was applied to the Pt top electrode, oxygen ions migrated to the top electrode while oxygen vacancies moved in the opposite direction toward the Pt bottom electrode. The oxygen vacancies were concentrated near the bottom electrode region and provided the basis for conducting filament formation, as shown in Fig. 8b. During the set process, as the electrons were supplied to the ZnO films, oxygen vacancies made up the conducting filaments, and the oxygen ions were pushed to the side, resulting in an LRS (Fig. 8c). On the other hand, during the reset process, oxygen ions returned to the oxygen vacancies of the filaments, leading to a filament gap between the ZnO and Pt top electrode. The conducting filaments were ruptured, resulting in an HRS (Fig. 8d).

To sum up, bipolar resistive switching is expected to occur through a local redox reaction between conducting filaments and the top Pt electrode, resulting in formation or rupture of the filament. It is almost certain that such conductive filament formation and rupture plays a key role in the resistive switching characteristics of the ZnO films.

CONCLUSIONS

The bipolar resistive switching characteristics of a Pt/ZnO/Pt structure, where a ZnO film grown at 300°C to 500°C was deposited using a MOCVD system, were investigated. Analysis of RBS data of the ratio of Zn to O atoms in the films showed them to be oxygen-poor $Zn_1O_{0.9}$ at 300°C, stoichiometric Zn_1O_1 at 400°C, and oxygen-rich $Zn_1O_{1.3}$ at 500°C. The presence of oxygen defects in the ZnO films was confirmed by PL and XPS. ZnO films grown at 300°C and 400°C exhibited asymmetric *I*–*V* curves, but the oxygen-rich ZnO film grown at 500°C did not exhibit *I*–*V* characteristics. The proposed switching mechanism model is based on conductive filaments consisting of oxygen vacancies and that the Pt electrode behaved as an oxygen reservoir. The bipolar switching behaviors may have been associated with redox-reaction-induced oxygen ions in the ZnO films.

REFERENCES

1. G.I. Meijer, *Science* 319, 1625 (2008).
2. S.Q. Liu, N.J. Wu, and A. Ignatiev, *Appl. Phys. Lett.* 76, 2749 (2000).
3. S. Seo, M.J. Lee, D.H. Seo, E.J. Jeoung, D.S. Suh, Y.S. Joung, I.K. Yoo, I.R. Hwang, S.H. Kim, I.S. Byun, J.S. Kim, J.S. Choi, and B.H. Park, *Appl. Phys. Lett.* 85, 5655 (2004).
4. S. Kim and Y.K. Choi, *IEEE Trans. Electron Devices* 56, 3049 (2009).
5. Y.H. Do, J.S. Kwak, Y.C. Bae, K. Jung, H. Im, and J.P. Hong, *Appl. Phys. Lett.* 95, 093507 (2009).
6. S.P. Heluani, G. Braunstein, M. Villafuerte, G. Simonelli, and S. Duhalde, *Thin Solid Films* 515, 2379 (2006).
7. N. Xu, L.F. Liu, X. Sun, X.Y. Liu, D.D. Han, Y. Wang, R.Q. Han, J.F. Kang, and B. Yu, *Appl. Phys. Lett.* 92, 232112 (2008).

8. N. Xu, L.F. Liu, X. Sun, C. Chen, Y. Wang, D.D. Han, X.Y. Liu, R.Q. Han, J.F. Kang, and B. Yu, *Semicond. Sci. Technol.* 23, 075019 (2008).
9. A. Sawa, *Mater. Today* 11, 28 (2008).
10. S.H. Jo, K.H. Kim, and W. Lu, *Nano Lett.* 9, 870 (2009).
11. F. Pan, C. Chen, Z.S. Wang, Y.C. Yang, J. Yang, and F. Zeng, *Prog. Nat. Sci.* 20, 1 (2010).
12. J.J. Yang, M.D. Pickett, X.M. Li, D.A.A. Ohlberg, D.R. Stewart, and R.S. Williams, *Nat. Nanotechnol.* 3, 429 (2008).
13. Y.R. Ryu, T.S. Lee, J.A. Lubguban, H.W. White, B.J. Kim, Y.S. Park, and C.J. Youn, *Appl. Phys. Lett.* 88, 241108 (2006).
14. Y.K. Tseng, C.J. Huang, H.M. Cheng, I.N. Lin, K.S. Liu, and I.C. Chen, *Adv. Funct. Mater.* 13, 811 (2003).
15. M.S. Arnold, P. Avouris, Z.W. Pan, and Z.L. Wang, *J. Phys. Chem. B* 107, 659 (2003).
16. W.Q. Yang, J. Chen, G. Zhu, X.N. Wen, P. Bai, Y.J. Su, Y. Lin, and Z.L. Wang, *Nano Res.* 6, 880 (2013).
17. Z.L. Wang and J.H. Song, *Science* 312, 242 (2006).
18. Q. Yang, Y. Liu, C.F. Pan, J. Chen, X.N. Wen, and Z.L. Wang, *Nano Lett.* 13, 607 (2013).
19. R.M. Yu, C.F. Pan, J. Chen, G. Zhu, and Z.L. Wang, *Adv. Funct. Mater.* 23, 5868 (2013).
20. W.Y. Chang, H.W. Huang, W.T. Wang, C.H. Hou, Y.L. Chueh, and J.H. He, *J. Electrochem. Soc.* 159, 29 (2012).
21. L.E. Greene, M. Law, J. Goldberger, F. Kim, J.C. Johnson, Y.F. Zhang, R.J. Saykally, and P.D. Yang, *Angew. Chem. Int. Ed.* 42, 3031 (2003).
22. J. Zhao, L. Hu, Z. Wang, Y. Zhao, X. Liang, and M. Wang, *Appl. Surf. Sci.* 229, 311 (2004).
23. G. Schön, *J. Electron Spectrosc. Relat. Phenom.* 2, 75 (1973).
24. P.T. Hsieh, Y.C. Chen, K.S. Kao, and C.M. Wang, *Appl. Phys. A* 90, 317 (2008).
25. D.S. Park, Y.J. Tak, J.Y. Kim, and K.J. Yong, *Surf. Rev. Lett.* 14, 1061 (2007).
26. M. Hecq, A. Hecq, J.P. Delrue, and T. Robert, *J. Less Common. Met.* 64, 25 (1979).
27. Y. Abe, H. Yanagisawa, and K. Sasaki, *Jpn. J. Appl. Phys.* 37, 4482 (1998).
28. T.G. Seong, M.R. Joung, J.W. Sun, M.K. Yang, J.K. Lee, J.W. Moon, J. Roh, and S. Nahm, *Jpn. J. Appl. Phys.* 51, 041102 (2012).